



A Facile Novel Synthesis of Cadmium oxide Nanoparticle Decorated Oleic acid with Enhanced Photocatalytic activity for the Degradation of Crystal Violet under Solar Light Irradiation

**A.Subalakshmi¹, B.Kavitha², N. Srinivasan³, M. Rajarajan⁴
A. Karthika⁵ and A. Suganthi^{5*}**

1. Department of Physics, C.P.A. College, Bodinayakanur-625513, Tamilnadu, **INDIA**
2. P.G. and Research Department of Chemistry, C.P.A. College, Bodinayakanur-625513, Tamilnadu, **INDIA**
3. P.G. and Research Department of Physics, Thiagarajar College, Madurai-625009, Tamilnadu, **INDIA**
4. Directorate of Distance Education, Madurai Kamaraj University, Madurai-625009, Tamilnadu, **INDIA**
5. P.G. and Research Department of chemistry, Thiagarajar College, Madurai-Tamilnadu, **INDIA**

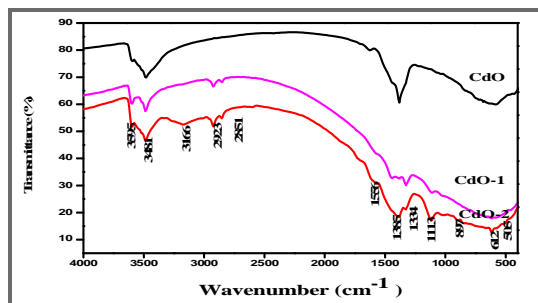
Email: vasan692000@yahoo.com, rajarajan_1962@gmail.com

Accepted on 19th November, 2019

ABSTRACT

Oleic acid coated CdO nanoparticles were synthesized using a facile, rapid, efficient and mild ultrasonic method. The structural, optical and surface morphological properties were proved by various techniques of X-ray diffraction (XRD), UV-Vis-Diffuse reflectance spectroscopy (UV-Vis-DRS), Fourier transform infrared spectroscopy (FT-IR), scanning electron microscopy (SEM) with an energy dispersive X-ray (EDX) spectroscopy and high resolution transmission electron microscope (HR-TEM). The X-ray diffraction (XRD) shows that face centered cube structure of oleic acid coated CdO and the average crystallite sizes were calculated to be 53.66 nm. FT-IR spectra confirmed the presence of metal oxides bands (band at 612 cm⁻¹ corresponds to CdO vibration) and the bands corresponding to oleic acid. The absorption maximum of CdO nanoparticles was shifted to visible region after coating of oleic acid. The visible light photocatalytic performances of the oleic acid coated CdO nanoparticles were evaluated by photodegradation of Crystal Violet dye as model organic pollutant. The result showed that oleic acid coated CdO (91 %) exhibited much higher visible light photocatalytic activity than CdO (75 %). As a result, it can be seen that the addition of oleic acid as a surface modifier improves the photocatalytic activity, prevents particle agglomeration and provides a very stable CdO nanoparticles.

Graphical Abstract



FT-IR spectrum of CdO, CdO-1 and CdO-2 NPs.

Keywords: CdO, Oleic acid, Photocatalysis, Crystal Violet, Solar light.

INTRODUCTION

Nano-photocatalysis is an important technology to solve the energy and environment related problems with the help of inexhaustible solar energy [1-3]. The environmental contaminant of water caused by organic and toxic waste has drawn more attention during the past several decades. Many usual methods such as catalytic reduction, osmosis and adsorption techniques have been used to deals with the pollutants in environmental surroundings. There are many drawbacks still exist in these methods such as increase in number of refractory pollutants and high expensive procedures [4]. Photocatalysis is considered to be most effective among the above methods applied for air and water treatment. In the area of heterogeneous photocatalysis metal oxide has involved a great deal of attention as an innovative catalytic material [5, 6].

Cadmium oxide nanostructures have received extensive concern due to their proficient properties for many technologies. Cadmium oxide powder is a brownish materials having a face-centred-cubic crystal structure among a lattice constant $a = 0.4695$ nm. The values of the band gap in the range 2.2 and 2.5 eV is reported used to room temperature n-type CdO nanostructure semiconductor [7, 8]. CdO nanoparticles are useful in gas sensors, photodiodes, solar cells, catalysts, photocatalysts and optoelectronic devices [9-11]. The several structures of cadmium oxide in nanoscale have been reported viz., nanoparticles, nanowires[12] thin films, nanoneedles, nanotube [13] and nanorods [14]. The techniques to prepare these materials to contain sonochemical [15], micro-emulsion [16], hydrothermal/solvothermal method and mechanochemical process [17]. Metal oxide semiconductor absorbs visible light radiation from sunlight. In a metal oxide, electrons from the valence band are transferred to the conduction band, creating electron–hole ($e^- - h^+$) pairs. At the surface of the nanoparticles, the electron and the holes can reduce and oxidized adsorbed from the environment oxygen and water molecules, respectively. Therefore superoxide ions and hydroxyl radicals can be generated on the metal oxide surface, whichever to the key species initiating the photocatalytic oxidation process [18, 19]. The stability and catalytic efficiency of metal oxide have been improved by a variety of techniques such as doping [20, 21] coupling with narrow band gap semiconductors [22, 23] and modification with surfactant [24, 25].

The surface modification of a catalyst by dye sensitization or colourless organics is a good chance to develop a method of designing a visible light reactive in photocatalytic system [26]. The colourless organic acid, surface-modified technique was re-designated as organic acid coated method [27,28]. Among the different colorless organics surfactants, oleic acid is an tremendous one because of its high resemblance to the surface of superfine magnetite. Oleic acid is the most general organic acids, featuring in esterification and surfactant chemistry. The carboxyl groups as of Oleic acid can form ester like linkage (C=O) or carboxylate linkage (C-O-O) with metal oxide, which played a positive role in the ret-shift of the absorption edge metal oxide nanoparticles [29, 30].

The photocatalytic activity of oleic acid modified CdO NPs under solar light has not been studied so far. In this report, CdO and oleic acid modified CdO NPs were synthesized by a co-precipitation method. Throughout synthesis, the amount and the rate of adding together of oleic acid were optimized to get required CdO nanostructures. The structural, morphology and optical properties of the as prepared CdO, oleic acid and oleic acid modified CdO NPs were investigated by XRD, FT-IR, UV-Vis-DRS, SEM, EDAX and HR-TEM. The present work demonstrated the excellent photocatalytic activity of the synthesized oleic acid modified CdO against crystal violet dye under solar light irradiation. Oleic acid, and tremendous surface modification agent, was usual to have optimistic effect in such synthesis. The improvement of such low cost and valuable photocatalysts is enviable for future applications in the field of photocatalysis.

MATERIALS AND METHODS

Materials: The chemicals of cadmium nitrate, ammonia and oleic acid are purchased from Merk with 99.95% purity and were used without further purification and highly purified deionized water.

Synthesis: An aqueous solution of suitable amount of $\text{CdNO}_3 \cdot 7\text{H}_2\text{O}$ (0.5M) was prepared. The prepared solution was stirred for two hour and afterwards ammonia solution was added drop wise until pH of the solution reaches 8.0. A white precipitate is formed due to addition of ammonia. The stirring of solution was continued for another 5hrs at room temperature. The final compound was kept to settle down for 1 day. After that the solution was filtered and washed with deionised water to take out unreacted materials. The obtained precipitate was dried at 100°C and then grinded to fine powder with mortar and pestle. The powder obtained was calcinated at 350°C for 3h to obtain final product [31]. The surface modification of CdO nanoparticles by oleic acid was conducted all the way through a sonochemical method with jealous the speed of water generation. The typical preparation route was as follows: 3 g of CdO NPs was added to 30 ml of ethanol kept in ultrasonic vibrator at 40 kHz for 30 min. In order to achieve the better dispersion of the NPs, the ultrasonic temperature was set at 45°C for 30 min. 1 mL and 1.5 mL of dispersed oleic acid 1 mL and 1.5 mL were taken in a round bottom flask separately and 30 mL of dispersed CdO was poured suddenly on to the solution (CdO-1 & CdO-2), stirred well for 3 h and allowed to sediment for 24 h and filtered. Then the precipitate of oleic acid coated CdO NPs were separated by centrifugation and washed with ethanol several times and then dried in hot air oven at 120°C for 5h.

Characterization: The XRD pattern as prepared samples were taken using an X-ray diffractometer (X'PERT PRO X- RAY) using $\text{Cu K}\alpha$ irradiation at 25°C and the peak assignment were made with reference to the JCPDS powder diffraction files. The Fourier transform infrared spectra (FTIR) were recorded with a JASCO Model 460 plus FT-IR spectrometer. The direct band gap of solid samples measured using UV-Vis diffuse reflectance spectroscopy (JASCO V-550) and the optical band gap of semiconductor was estimated using Tauc plot. The surface morphology of the prepared samples was studied by using scanning electron microscope (JSM-6701F-6701) and also analyzed the chemical element. High resolution transmission electron microscopy and corresponding selected –area electron diffraction (HR-TEM/SAED) was carried out on a transmission electron microscope (TEM-TECNAI G2 model). Photocatalytic experiments were carried out in an immersion type photoreactor (HPR-Compact-p-8/125/250/400).

Measurement of Photodegradation of CV: The photoactalytic experiments were carried out at the natural pH of CV (Crystal Violet) dye solution. The photocatalytic activities of the as synthesized CdO-1 & 2 NPs were evaluated by photodegradation of CV (30 μM) dye under solar light irradiation. 300 ml of aqueous solution of CV was taken in a round bottom flask. Then, photocatalyst was added to the CV solution, the catalyst concentration was fixed 0.1g L^{-1} , subsequently, the mixture was stirred in the dark for about 30 min to maintain equilibrium between adsorption and desorption. The resulting suspension was irradiated under direct sunlight at the time interval between 11.00 AM to 2.30 PM. by placing on the top roof of our laboratory, Bodinayakanur, Tamilnadu, India during summer (April–May). The solutions were stirred continuously and open to air environment. During the solar light irradiation, 5 mL of sample was taken out from the suspension at a defined time interval. The photocatalyst was separate by centrifugation and the left over CV concentration was analyzed using a UV-Vis Spectrometer (λ_{max} of CV 582 nm). The photolysis experiments were also carried out at by the same process described over without catalyst.

The photo-degradation percentage of crystal violet was calculated using the formula given below [32]:

$$\text{Photo-degradation (\%)} \text{ efficiency} = [(C_0 - C)/C_0] * 100$$

Where C_0 is the initial concentration of crystal violet before irradiation and C is the concentration of crystal violet after a certain irradiation time.

RESULTS AND DISCUSSION

X-Ray diffraction: The crystal structures of the as prepared CdO, CdO-1 and CdO-2 NPs are elucidating by XRD analysis as shown in [figure1](#). It confirms a face centered cubic structure of CdO with value of lattice constant ‘ a ’=4.6946 Å [JCPDS 75-0592]. The diffraction peaks observed at 32.48° , 37.78° , 55.74° , 65.45° and 68.67° corresponds to the plane values of 111, 200, 220, 311, and 222 respectively. The sharp intensity of each diffraction peak indicates that the synthesized CdONPs possess good crystallinity [33] as shown in [figure 1](#). The lattice constant (a) was calculated using the standard formula

$$d = \frac{a}{\sqrt{h^2 + k^2 + l^2}}$$

Where d is the inter planer spacing and h , k , l are the Miller indices.

The average crystalline size of the NPs was determined using the Scherrer relation [34] eq (1) on 111 plane of X-ray diffraction pattern

$$D_{hkl} = k \lambda / \beta \cos\theta \quad \text{-- (1)}$$

Where D is the average crystalline size, λ is the X-ray wavelength, β is full width at half maximum (FWHM) and θ is the Bragg diffraction angle. The crystallite sizes of CdO, CdO-1 and CdO-2 are found to be 48.27 nm, 53.35 nm and 57.92 nm. The crystallite sizes of the nanocomposites are higher than that of CdO. This is ascribed to the nanodeposition of oleic acid on the surface of CdO.

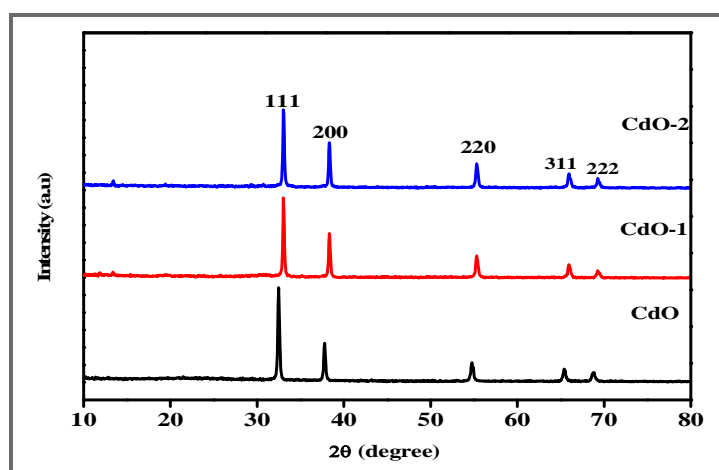


Figure 1. XRD patterns of CdO, CdO-1 and CdO-2 NPs.

FT-IR: The FT-IR spectrum of CdO and oleic acid coated CdO NPs is recorded in the spectral range of 4000 to 400 cm^{-1} and the results are displayed in [figure 2](#). The strong absorption band centered at $\sim 3481 \text{ cm}^{-1}$ and 3595 cm^{-1} is assigned to the $-\text{OH}$ stretching vibrations of hydroxyl group [35]. It has been reported that the strong IR bands around ~ 500 , ~ 1000 , 1400 cm^{-1} are the characteristic bands of CdO [36-38]. A strong absorption band observed at 1385 cm^{-1} is due to wagging vibrations of C-H group. The characteristic peaks adsorption at 612 cm^{-1} confirms the formation of CdO. In addition, the peaks at 3481 and 1556 cm^{-1} are the H_2O characterized absorbing peaks. The oleic acid coated CdO particles showing bands at 2923 and 2851 cm^{-1} are due to $-\text{CH}_3$ and $-\text{CH}_2$ vibration respectively [39],

40] reveal that the two oxygen atoms in the carboxylate group of oleic acid are co-ordinated on the surface of the particle.

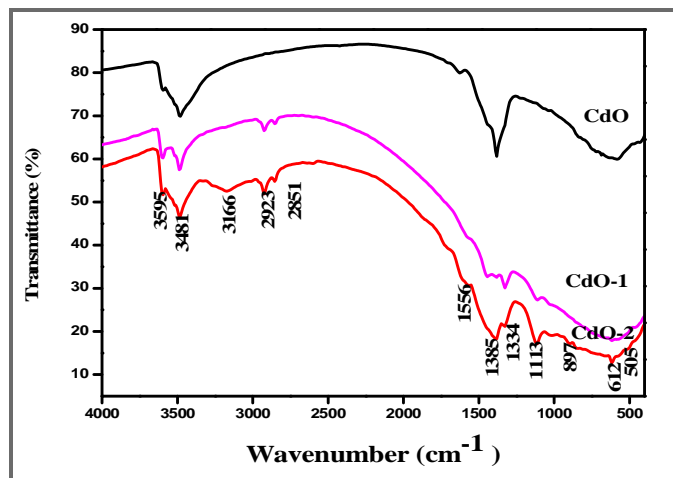


Figure 2 .FT-IR spectrum of CdO, CdO-1 and CdO-2 NPs.

UV-Vis DRS: In order to study the absorption behavior of synthesized samples UV-Vis spectra for CdO, CdO-1 and CdO-2 NPs were recorded in the spectral range 200 to 800 nm as shown in figure 3. From the Figure, the spectrum it can be seen that pure CdO shows maximum absorption at 483 nm. The CdO-NPs show a red shift. The band gap energies were calculated using the Tauc relation

$$\alpha h\gamma = A (h\gamma - E_g)^n \quad \text{-- (2)}$$

Where A is an energy-independent constant, α is the absorption coefficient, h is the planck's constant, γ is the frequency of vibration, E_g is the optical band gap and the value $n=1/2$ or 2, for direct and indirect allowed transitions respectively [41]. The tauc plot $(\alpha h\gamma)^2$ vs $h\gamma$ was plotted for CdO, CdO-1 and CdO-2 NPs shown in figure 4 a, b and c respectively. The optical band gaps were found to be 2.02 eV, 1.84eV, and 1.74eV for CdO, CdO-1 and CdO-2 respectively.

The decrease in band gap of CdO from 2.10eV to 1.74eV, after the surface modification of CdO-1 and CdO-2 NPs, indicate the electronic transition between the two components. The change in absorption edge and band gap of CdO testifies that the surface is successfully modified with oleic acid. UV-Vis-DRS result infers that the synthesized NPs could absorbs more visible light under stimulated solar light irradiation.

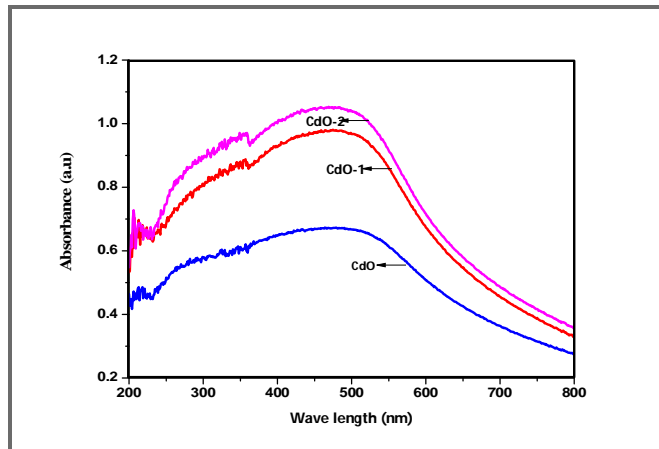


Figure 3. UV- Vis spectra of CdO, CdO-1 and CdO-2.

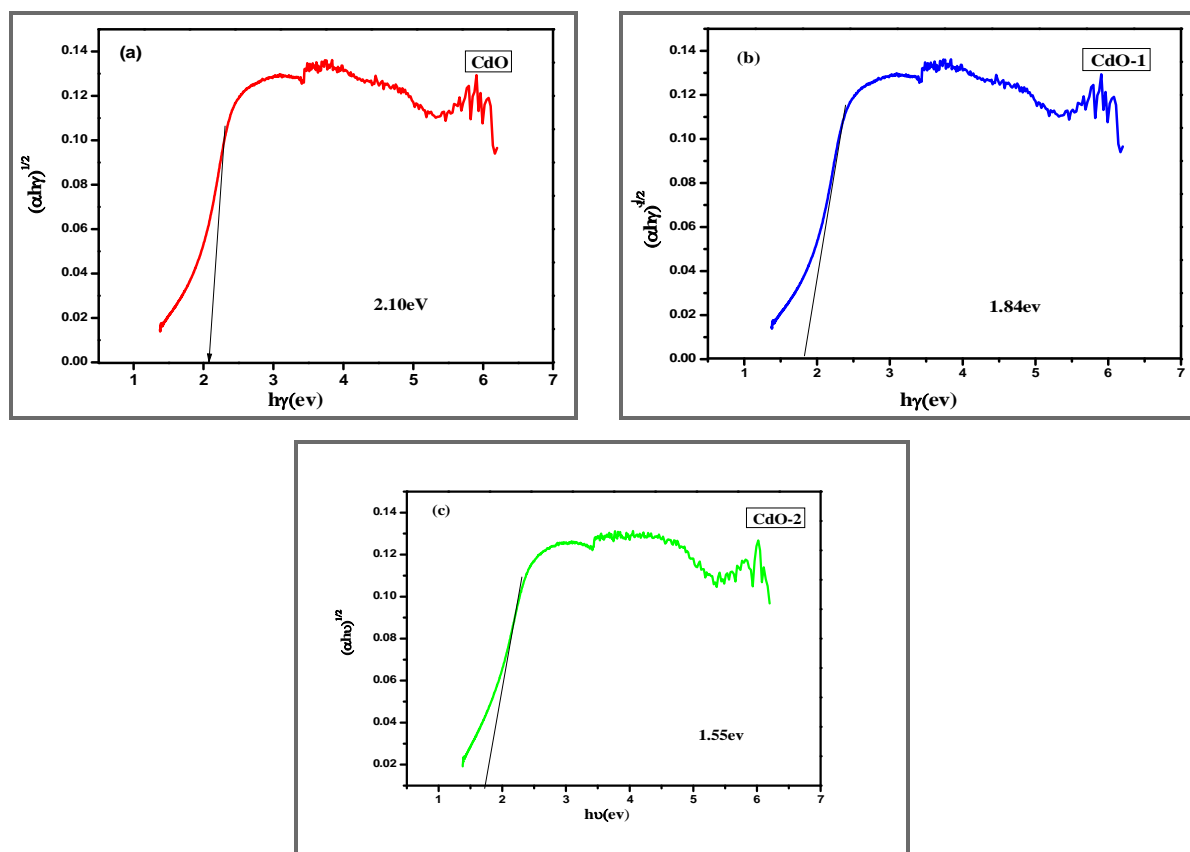


Figure 4.Tauc plot of CdO (a), CdO-1 (b) and CdO-2(c)

SEM- EDX: The SEM micrographs of CdO, CdO-1and CdO-2 NPs were as shown in figure 5(a),(b) and (c). From figure 5(a) CdO sample is formed by low tense agglomeration homogeneous distribution and CdO-1, CdO-2 shows needle with rod like aggregates structure. The EDX spectrum of CdO NPs confirms the presence of cadmium and oxygen in their normal energy values (Figure 5(d)).

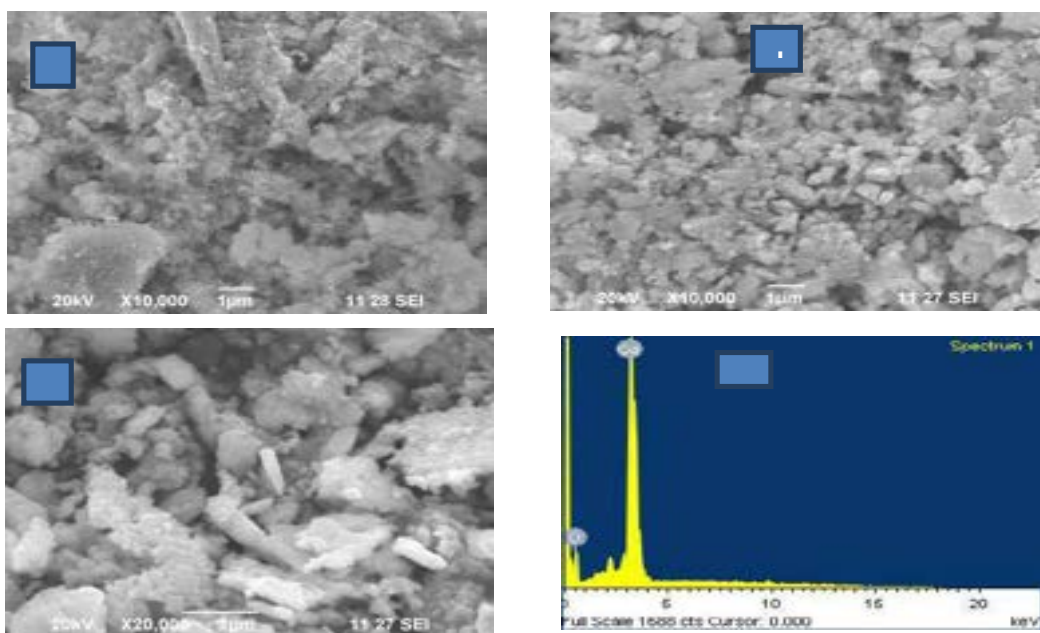


Figure 5. (a)SEM image of CdO, (b)CdO-1, (c) CdO-2 and (d)EDX spectrum.

HR-TEM-SAED: The HR-TEM images of the synthesized oleic acid coated with CdO NPs were shown in figure 6(a). The average diameter of oleic acid coated CdO NPs appears to be \sim 56 nm. It is in good agreement with crystalline values calculated using XRD results. In the current study, oleic acid was used as stabilizer for the formation of well defined CdO NPs. Figure 6(b) shows that the finger fringes of oleic acid coated CdO NPs. The selected area electron diffraction (SAED) pattern was displayed in figure 6(c). The pattern shows three strong diffraction rings corresponding to the (111), (200) and (220) planes, which is in agreement with the cubic structure corresponding to the XRD results.

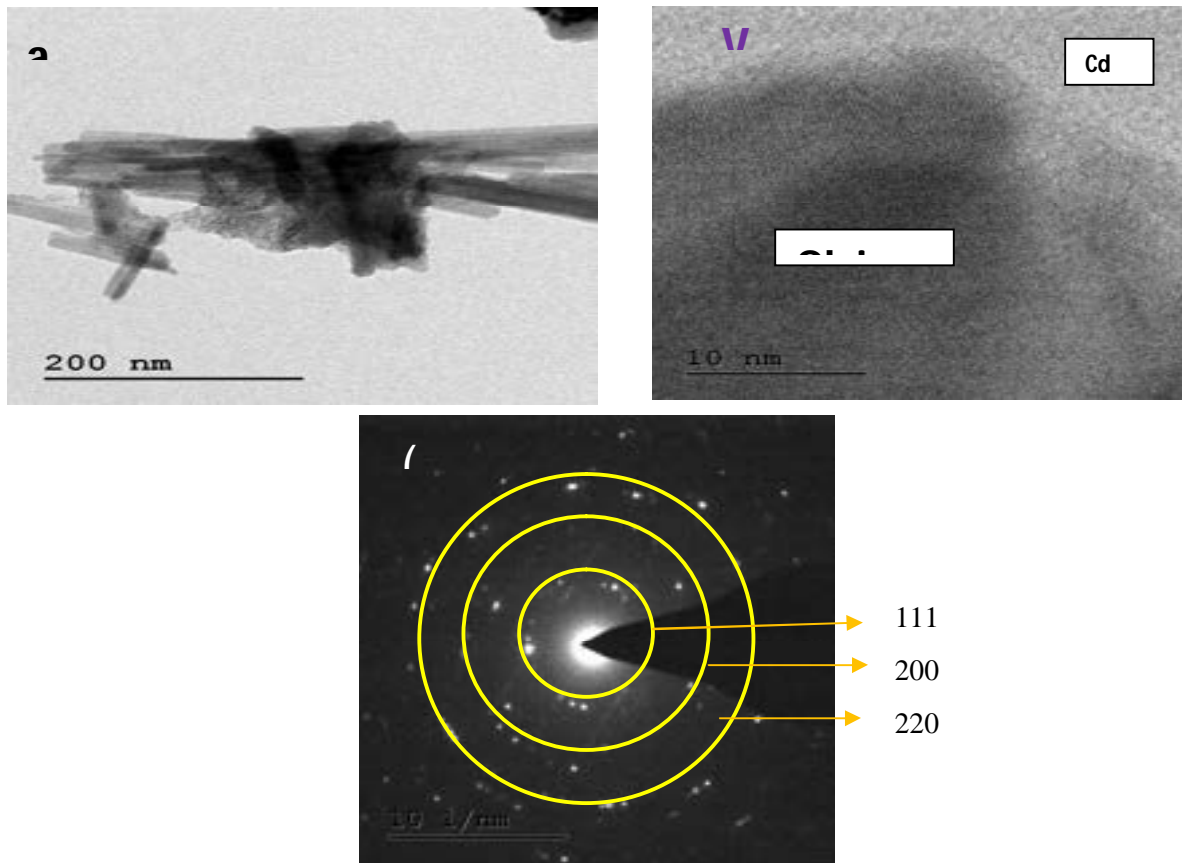


Figure 6. (a) HR-TEM image (b)finger fringes and (c) SAED pattern of of Oleic acid coated CdO NPs.

Photocatalytic Activity: The photocatalytic activity of the as prepared samples of CdO, CdO-1 and CdO-2 was evaluated for the degradation of CV under solar light irradiation. The changes in the UV-Vis spectra of CV (30 μ M) in the presence of CdO-2 (0.1g L^{-1}) under solar light irradiation at pH 3 are displayed in figure 7(a). The decrease in the absorbance intensity of CV at λ_{max} (583 nm) is indicated by the degradation of dye [42]. Figure 7(b) shows the photo-degradation of CV as a function of irradiation time over CdO, CdO-1 and CdO-2. It is important to note that the contact time prior to irradiation was 30 min. for all the samples and it was 180 min. during the CV photodegradation. CdO-2 exhibits higher photocatalytic activity (91%) among CdO and CdO-1.

Photodegradation of kinetics of CV: The photodegradation kinetics of CV using the as-synthesized catalysts was investigated by applying Langmuier-Hinselwood model

$$-\ln (C/C_0) = kt \quad \text{--(3)}$$

Where C_0 is the initial concentration of dye, C the concentration of the dye in the reaction time and k is the pseudo first order rate constant. The linear fitting curves of $-\ln (C/C_0)$ versus irradiation time are

plotted in figure 7(c). The observed rate constant (k) for the photocatalytic degradation of CV were evaluated from experimental data using a linear plot. It is observed that the ' k ' value of CdO-2 determined was $1.01 \times 10^{-2} \text{ S}^{-1}$ which is significantly higher than that of CdO ($0.2 \times 10^{-2} \text{ S}^{-1}$) and CdO-1 ($0.410^{-2} \text{ S}^{-1}$).

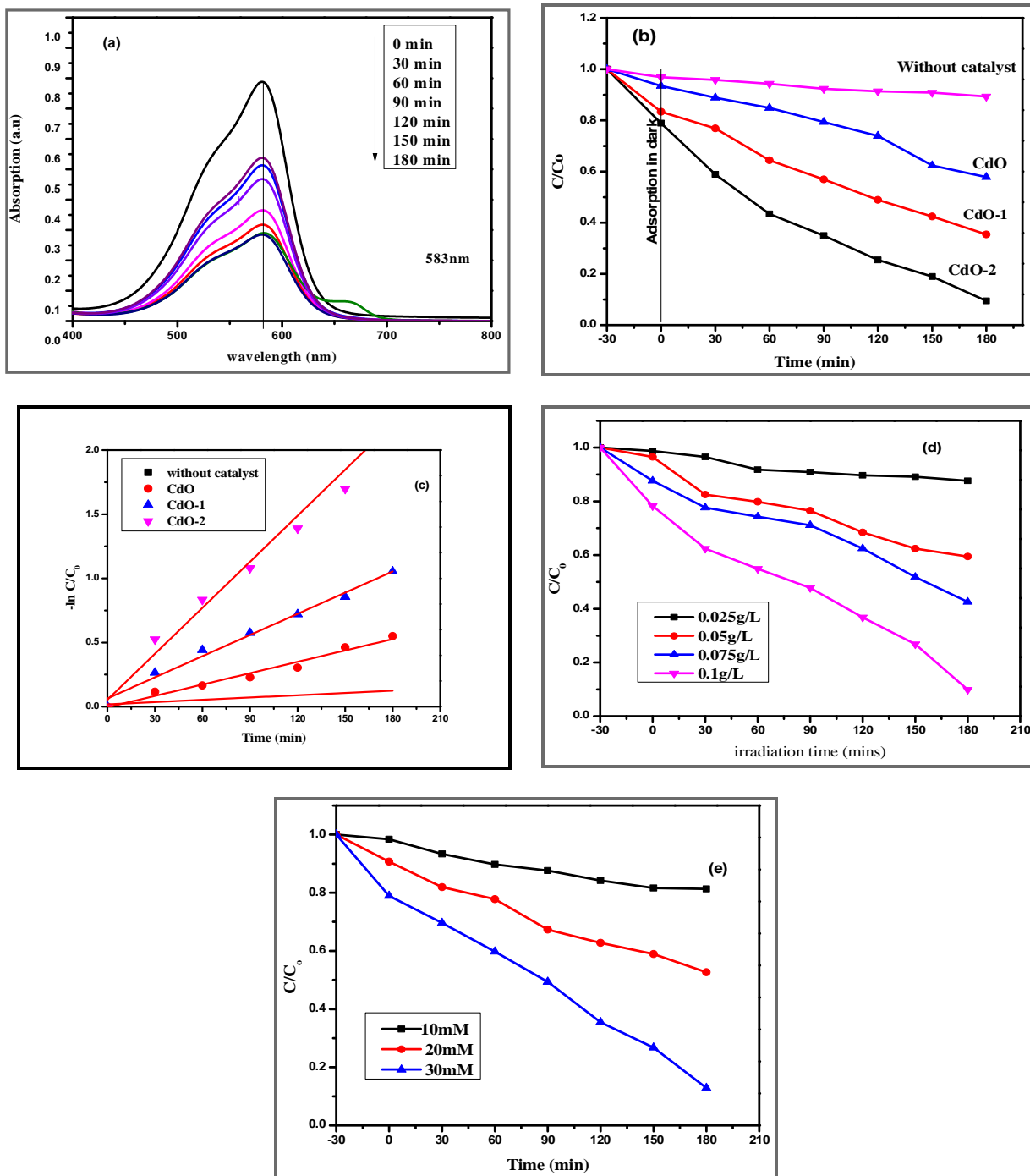


Figure 7. (a) UV-Vis absorption changes of CV ($30 \mu\text{M}$) in the presence of CdO-2 (0.1 g L^{-1}) under simulated solar light irradiation. (b) Photodegradation of CV using various photocatalyst. (c) Kinetics of CV Photodegradation for different catalyst. (d) Effect of catalyst concentration on the Photodegradation of CV. (e) Effect of initial CV concentration on the Photodegradation.

Effect of catalyst concentration: The quantity of catalyst in photocatalytic process is significant as it can strongly influence the degradation effect. The photocatalytic experiments were conducted by

varying CdO-2 concentration as 0.025, 0.05, 0.075, 0.1 g L⁻¹ and observance the other parameters constant. The results are represented in figure 7(d). The photodegradation of CV increasing the catalyst from 0.025 g L⁻¹ to 0.1 g L⁻¹ and a further increment in catalyst absorption leads to reduce in photodegradation. This is owing to the increase of total active surface area and the convenience of extra dynamic sites on the catalyst surface for photoreaction. But the photocatalytic activity decreases at high catalyst concentration due to overlapping of surface dynamic sites.

Effect of initial dye concentration: The effect of initial CV concentration on the photodegradation is investigated at three initial dye concentrations of 10, 20, and 30 μ M as a function of irradiation time in the presence of 0.1g L⁻¹ of CdO-2 at pH 3. The results are shown in figure 7(e). The photo degradation of CV increases with increases in CV concentration. As the initial CV concentration increases, the degradation percentage decreases. Since the following reasons: at high dye concentration, the generation of active species on the photocatalyst surface is reduced as the active sites are absolutely covered by the dye molecules. According to Beer–Lamberts law the path length of photons entering into the dye solution decreases. The generation of reactive species also remains constant at fixed catalyst concentration.

Photocatalysis mechanism of Oleic acid modified CdO: Here, we propose a possible photocatalysis mechanism for the OC-modified CdO, as shown in figure 8. This photocatalytic degradation mechanism contains these four steps: (i) the visible light irradiation on CdO surface improved by the OC, (ii) the excitation of e⁻ from valance band (VB) to the conduction band (CB) of CdO, and leaving the h⁺ in VB, (iii) the e⁻ and h⁺ firstly reacts with H₂O, and (iv) then induced the degradation of organic pollutants.

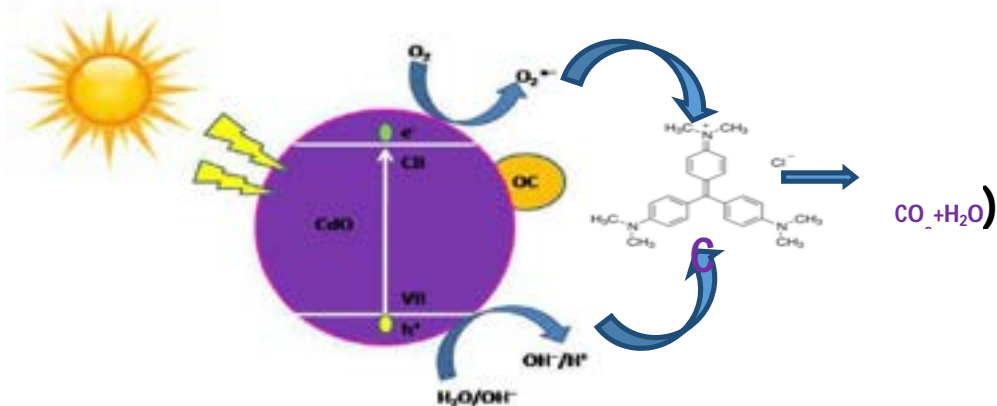


Figure 8. The schematic diagram of electron–hole transfer process in Oleic acid modified CdO under solar light irradiation.

Reusability studies: The photocatalytic reusability and stability of CdO-2 NPs was evaluated by cyclic experiments. Three cycles of CV degradation tested using CdO-2 as photocatalyst for 180 min of light irradiation. The results are shown in figure 9. The CV dye is quickly washed-out after each CV decomposition experiments, and CdO-2 photocatalysts are stable throughout the cyclic experiments with no exhibiting any considerable loss of photocatalytic activity. As a result the prepared CdO-2 NPs could be regarded as a effective photocatalysts for the degradation of CV.

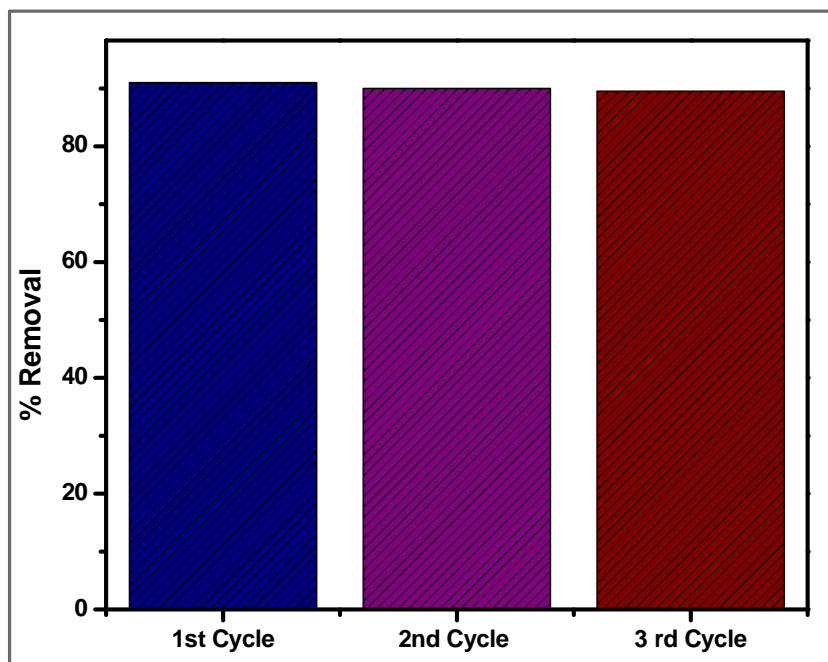


Figure 8. Reusability of different cycle of CdO-2 NPs.

CONCLUSION

Using a simple, mild and cost effective coprecipitation method of synthesis of Oleic acid coated CdONPs, the structural and optical properties were investigated. The observed XRD peaks with sharp intensity confirm impurity free and the crystalline nature of CdO NPs. The band gap energy was calculated using UV-Vis-DRS spectrometer. The FT-IR spectroscopic method confirmed the presence of functional groups. The morphology and size of the nanoparticles were observed by SEM and HR-TEM analysis respectively. CdO, CdO-1 and CdO-2 has been synthesized and effectively utilized as a solar light driven photocatalyst for the degradation of CV. During 3 h of solar light irradiation, 91% of CV is degraded using 0.1 g L⁻¹ of CdO-2. The results of this research work testify that CdO-2 will act as a promising photocatalyst for the degradation of organic dyes in aqueous environment.

REFERENCES

- [1]. S. M. Lam, J. C. Sin, A. Z. Abdullah, A. R. Mohamed, Transition metal oxide loaded ZnO nanorods: Preparation, characterization and their UV–Vis photocatalytic activities Sep, *Purif. Technol.*, **2014**, 132, 378-387.
- [2]. X. Feng, H. Guo, K. Patel, H. Zhou, X. Lou, High performance, recoverable Fe₃O₄ ZnO nanoparticles for enhanced photocatalytic degradation of phenol, *J.Chem.Eng.*, **2014**, 244,327-334.
- [3]. H.S. Kim, D. Kim, B.S. Kwak, G.B. Han, M.-H. Um, Kang, Synthesis of magnetically separable core@shell structured NiFe₂O₄@TiO₂ nanomaterial and its use for photocatalytic hydrogen production by methanol/water splitting, *J.Chem. Eng.*, **2014**, 243, 272-279.
- [4]. K. Qi, F. Zasada, W. Piskorz, P. Indyka, J. Grybos, M. Trochowski, M. Buchalska, 480 M.Kobielusz, W. Macyk, Z. Sojka, Self-Sensitized Photocatalytic Degradation of Colorless Organic Pollutants Attached to Rutile Nanorods—Experimental and Theoretical DFT+D Studies, *J. Phys. Chem. C*, **2016**, 120, 5442-5657.
- [5]. N. Serpone, E. Pelizzetti and H. Hidaka, in: D. F. Ollis, H. A1-Ekabi (Eds.), Photocatalytic Purification and Treatment of Water and Air, Elsevier Science B.V., Amsterdam, **1993**, 225-250.

[6]. R.Satheesh, K.vignesh, A.Suganthi, M. RajarajanVisible light responsive photocatalytic applications of transition metal (M = Cu, Ni and Co) doped α -Fe₂O₃ nanoparticles, *J. Environ Chem .Eng.*, 2014, 2, 1956-1968.

[7]. A. Karthika, V. R. Raja, P. Karuppasamy, A. Suganthi, M. Rajarajan, A novel electrochemical sensor for determination of hydroquinone in water using FeWO₄/SnO₂ nanocomposite immobilized modified glassy carbon electrode, *Arabian Journal of Chemistry*, 2019.

[8]. N. Matsuura, D. J. Johnson, D. T. Amm, Fabrication of cadmium oxide thin films using the Langmuir-Blodgett deposition technique, *Thin Solid Films*, 1997, 295, 260-265.

[9]. X. Liu, C. Li, S. Han, J. Han, C. Zhou, Synthesis and electronic transport studies of CdO Nanoneedles, *Appl.Phys.Lett.*, 2003, 82, 1950-1952.

[10]. F. Yakuphanoglu, M. Caglar, Y. Caglar, S. Ilican, Electrical characterization of nanocluster n-CdO/p-Si heterojunction diode, *J. Alloys Comp.*, 2010, 506, 188–193.

[11]. K. Kaviyarasu, E. Manikandan, P. Paulraj, S. Mohamed, J. Kennedy, One dimensional well-aligned CdO nanocrystal by solvothermal method, *J.Alloys Comp.*, 2014, 593, 67-70.

[12]. P. Gadennc, Y. Yagil, G. J. Deutscher, Transmittance and reflectance in situ measurements of semicontinuous gold films during deposition, *Appl.Phys.*, 1989, 66, 3019.

[13]. Z. L. WangNanobelts, nanowires, and nanodiskettes of semiconducting oxides-from materials to nanodevices, *Advanced Materials*, 2003, 627, 432-436.

[14]. R. J. Bandraranayake, G. W. Wen, J. Y. Lin, H. X. Jiang, C. M. Sorensen, Structural phase behavior in II–VI semiconductor nanoparticles, *Appl.Phys.Lett.*, 1995, 67, 831-833.

[15]. S. H. Tolbert and A. P. Alivisators, The wurtzite to rock salt structural transformation in CdSe nanocrystals under high pressure, *J.chem.phys.*, 1995, 102, 4642 -4656.

[16]. N. Herron, Y. Wang, H. Eckert, Synthesis and characterization of surface-capped, size-quantized cadmium sulfide clusters. Chemical control of cluster size, *J.Am. Chem.soc.*, 1990, 1129, 322-1326.

[17]. G. Chiu, E. J. Meehan, The preparation of monodisperse lead sulfide sols, *J.Colloid Interface Sci.*, 1974, 49, 160.

[18]. D. Bahnemann, J. Cunningham, M. A. Fox, E. Pelizzetti, P. Pichat, N. Serpone, G. Helz, R. Zepp, D. Crosby, in: G. R. Heltz, R. G. Zepp, D. G. Crosby (Eds), Photocatalytic treatment of water. Aquatic and Photochemistry, *Lewis Publishers, Boca Raton, FL*, 1994, 261-552.

[19]. Y. Nosaka, Y. Yamashita H. Fukuyama, Application of Chemiluminescent Probe to Monitoring Superoxide Radicals and Hydrogen Peroxide in TiO₂ Photocatalysis, *J. Phys. Chem. B*, 1997, 101, 5822-5827.

[20]. K. Vignesh, M. Rajarajan, A. Suganthi, Visible light assisted photocatalytic performance of Ni and Th co-doped ZnO nanoparticles for the degradation of methylene blue dye, *J. Ind. Eng. Chem.*, 2014, 20, 3826–3833.

[21]. M.-H. Hsu, C.-J. Chang, Ag-doped ZnO nanorods coated metal wire meshes as hierarchical photocatalysts with high visible-light driven photoactivity and photostability, *J. Hazard. Mater.*, 2014, 278, 444–453.

[22]. H. Liu, X. He, Y. Hu, X. Liu, H. Jia, B. Xu, One-step hydrothermal synthesis of In₂O₃–ZnO heterostructural composites and their enhanced visible-light photocatalytic activity, *Mater. Lett.*, 2014, 131, 104–107.

[23]. X. Wang, X. Wan, X. Xu, Chen, Facile fabrication of highly efficient AgI/ZnO hetero junction and its application of methylene blue and rhodamine B solutions degradation under natural sunlight , *Appl. Surf. Sci.*, 2014, 321, 10–18.

[24]. M. Ahmad, E. Ahmed, Z.L. Hong, J.F. Xu, N.R. Khalid, A. Elhissi, W. Ahmed, A facile one-step approach to synthesizing ZnO/graphene composites for enhanced degradation of methylene blue under visible light, *Appl. Surf. Sci.*, 2013, 274, 273–281.

[25]. L. Sun, R. Shao, L. Tang, Z. Chen, Synthesis of ZnFe₂O₄/ZnO nanocomposites immobilized on graphene with enhanced photocatalytic activity under solar light irradiation, *J. Alloys Compd.*, 2013, 564, 55–62.

[26]. F. Chen, W. Zou ,W. Qu, J. Zhang, Photocatalytic performance of a visible light TiO_2 photocatalyst prepared by a surface chemical modification process, *Catal Commun.*, **2009**, 10, 1510–1513.

[27]. S. Li, W. Liang, F. Zheng, X. Lin, Visible Light-Driven Photocatalytic Activity of Oleic Acid-Coated TiO_2 Nanoparticles Synthesized from Absolute Ethanol Solution, *J. Cai, Nanoscale*, **2014**, 6, 14254–14261.

[28]. M. Jafarpour, Rezaeifard, M. Ghahramaninezhad, F. FeizpourDioxomolybdenum (VI) complex immobilized on ascorbic acid coated TiO_2 nanoparticles catalyzed heterogeneous oxidation of olefins and sulfides, *Green Chem.*, **2015**, 17, 442–452.

[29]. N. Nakayama ,T. Hayashi, Preparation of TiO_2 nanoparticles surface-modified by both carboxylic acid and amine: Dispersibility and stabilization in organic solvents, *A Colloids Surf Physicochem Eng Asp*, **2008**, 317, 543–550

[30]. U. Sulaeman, S. Yin, T. Sato, Visible light photocatalytic activity induced by the carboxyl group chemically bonded on the surface of SrTiO_3 . *Appl Catal B: Environ.*, **2011**, 102, 286–290

[31]. S. Kumar, B. Ahmed, K. Animesh. O. Jayanta Das, A. Kumar, Facile synthesis of CdO nanorods and exploiting its properties towards supercapacitor electrode materials and low power UV irradiation driven photocatalysis against methylene blue dye, *Materials Reserch Bulletin*, **2017**, 90, 224-231.

[32]. S. Kumar, A. Kumar, Chemically derived luminescent graphene oxide nanosheets and its sunlight driven photocatalytic activity against methylene blue dye, *Opt. Mater.*, **2016**, 62, 320–327.

[33]. S. Kumar, A. K. Ojha, B. Walkenfort, Cadmium oxide nanoparticles grown in situ on reduced graphene oxide for enhanced photocatalytic degradation of methylene blue dye under ultraviolet irradiation, *J. Photochem. Photobiol. B Biol.*, **2016**, 159, 111–119.

[34]. R. Henríquez, P. Grez, E. Muñoz, E.A. Dalchiele, R.E. Marotti, H. Gómez, Template-free non-aqueous electrochemical growth of CdO nanorods, *Thin Solid Films*, **2011**, 520, 41–46.

[35]. N. C. S. selvam, R. T. Kumar, K. Yogeenth, L. J. Kenndy, G. Selaran, J. J. VijayaSimple and rapid synthesis of Cadmium Oxide (CdO) nanospheres by a microwave-assisted combustion method. *powder Technol*, **2011**, 21, 250-255.

[36]. M. Ristic, S. Popvic, S. Music, Formation and properties of $\text{Cd}(\text{OH})_2$ and CdO particles, *Mater Lett.*, **2004**, 58, 2494-2499.

[37]. A. Askarinejad, A. Morsali, Synthesis and characterization of CdCO_3 and CdO nanoparticles by using a sonochemical method, *Matter Lett.*, **2008**, 62, 478–482.

[38]. M. Mazaheritenrani, J. Asghari, R. L. orimi, S. Pahlan, Microwave-Assisted Synthesis of Nano-Sized Cadmium Oxide As a New and Highly Efficient Catalyst for Solvent Free Acylation of Amines and Alcohols, *Asian J. Chem.*, **2010**, 22 , 2554-2564.

[39]. Q. Dai, M. Lam, S. Swanson, R. H. R. Yu, D. J. Milliron, T. Topuria, P. O. Jubert, A. Nelson, Monodisperse cobalt ferrite nanomagnets with uniform silica, *ACS J. Surf. Colloids*, **2010**, 26, 17546-17551.

[40]. X. M. Wang, C. N. Zhang, X. L. Wang, H. C. Gu, The study on magnetite particles coated with bilayer surfactants, *Appl. Surf. Sci.*, **2007**, 253, 7516-7521.

[41]. A. Karthika, S. Selvarajan, P. Karuppasamy, A. Suganthi, M. Rajarajan, A novel highly efficient and accurate electrochemical detection of poisonous inorganic Arsenic (III) ions in water and human blood serum samples based on SrTiO_3/β -cyclodextrin composite, *Journal of Physics and Chemistry of Solids*, **2019**, 127, 11-18.

[42]. S. Kumar, S. Layek, M. Yashpal, A. K. Ojha, Room temperature ferromagnetism in undoped and Mn doped CdO nanostructures, *J. Magn. Magn. Mater.*, **2015**, 393, 555–561.

[43]. Alireza Nezamzadeh-Ejhieh, Zohreh Banan, A comparison between the efficiency of CdS nanoparticles/zeolite A and $\text{CdO}/\text{zeolite A}$ as catalysts in photodecolorization of crystal violet, *Desalination* , **2011**, 279, 146–151.